UCRL-ID-123902

Liquid First Walls for Magnetic Fusion Energy

Ralph W. Moir

March 28, 1996

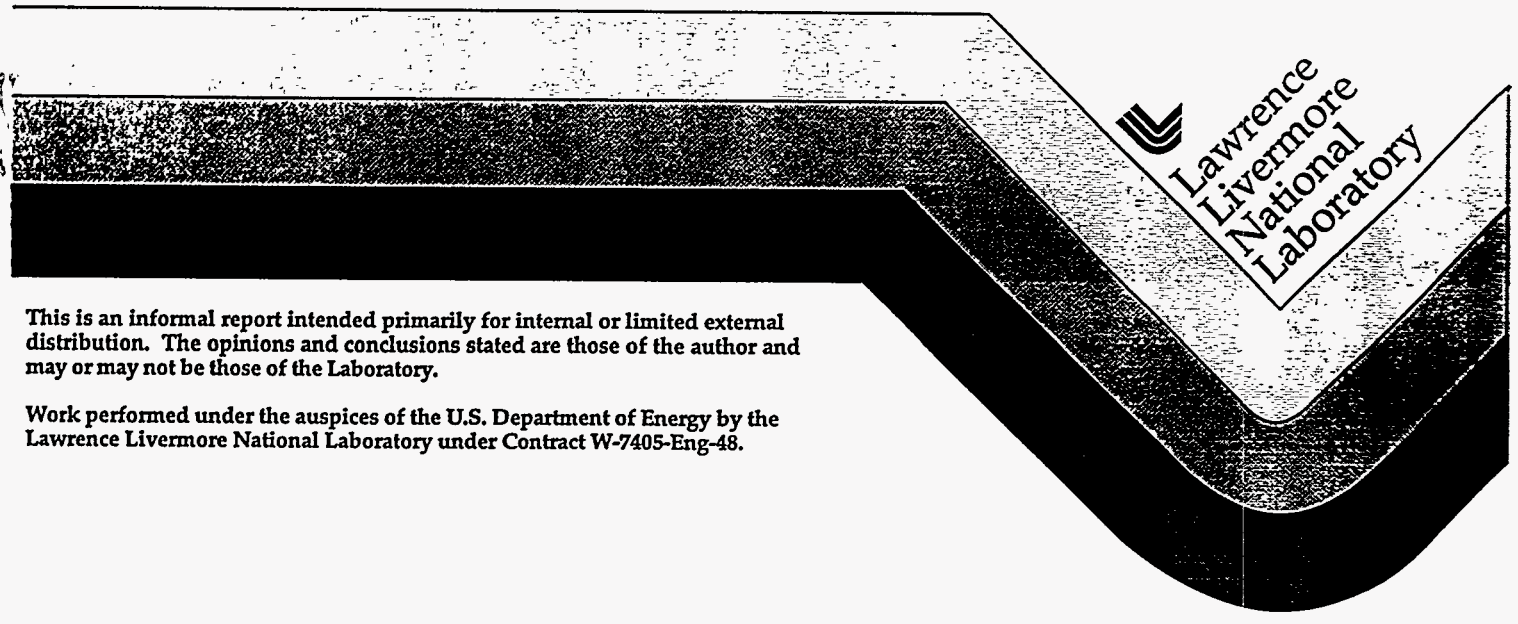

Work performed under the auspices of the U.S. Department of Energy by the Lawrence Livermore National Laboratory under Contract W-7405-Eng-48.

UCRL-ID-123902

Liquid first walls for magnetic fusion energy

Ralph W. Moir

March 28, 1996

Lawrence Livermore National Laboratory
P. O. Box 808, L-637
Livermore, California, 94551

Abstract

Liquids (~7 neutron mean free paths thick) with certain restrictions can probably be used in magnetic fusion designs between the burning plasma and the structural materials of the plant. If this works there are a number of profound advantages: lower the cost of electricity by more than 35%; remove the need to develop first wall materials saving over 4B$ in development costs; reduce the amount and kind of wastes generated in the plant; and permit a wider choice of materials. Evaporated liquid must be efficiently ionized in an edge plasma to prevent penetrating into the burning plasma and diminishing the burn rate. The fraction of evaporated material ionized is estimated to be 0.993 for Li, 0.98 for Flibe and 0.9999 for $Li_{17}Pb_{83}$. This ionized vapor would be swept along open field lines into a remote burial chamber. The most practical systems would be those with topological open field lines on the outer surface as is the case of a field reversed configuration (FRC), a Spheromak, a Z-pinch, or a mirror machine. In a Tokamak, including the Spherical Tokamak, the field lines outside the separatrix are restricted to a small volume inside the toroidal coil making for difficulties in introducing the liquid and removing the ionized vapor.

Introduction

The idea of replacing solid first walls with liquid walls for magnetic fusion was suggested by Christofilos[1] in 1971 and later a review of the idea was written[2] and updated recently[3]. The liquids can flow along field lines for conducting liquids (Li, $Li_{17}Pb_{83}$) or across field lines if the voltages generated do not cause too much current to flow with its resulting retarding force. A non conducting liquid such as the molten salt, Flibe, can flow across the field lines. With spinning containers more freedom is provided the designer and all three liquids that can breed tritium are candidates: Li, Flibe and $Li_{17}Pb_{83}$. Much of the information developed for liquids for the first wall might also be useful for liquid divertors[4], however, the focus of the present work is on the first wall and blanket which seems to be more demanding and the rewards are stupendously higher. In the Inertial Fusion Energy (IFE) application[3] use of liquids to protect the walls are in most cases essential. Use of thick liquids has been shown to save >30% in the cost of electricity for IFE[5]. In magnetic fusion the savings should be even more by allowing higher power density thus reducing magnet size and cost. This big of a savings if realizable would be most welcome. In my opinion, magnetic fusion energy (MFE) may very well not be a success without liquid walls. Liquid walls with their full ramification might make the difference between a workable but expensive and high waste generating power plant and one that is lower in cost than the competition and cleaner.

Liquid ($LiBeF_3$) walls for Tokamak geometry have been discussed in ref. 2 and 6 and is shown in Fig 1. In this case a liquid droplet jet is used to remove heat from the edge plasma similar to that of ref. 4. Specially designed penetrating nozzles would have to be periodically replaced. This design should be revisited with liquid lithium which would, however, have complicated MHD effects to consider.

For illustrative purposes the geometry used for the examples in this work will be that shown in Fig. 2 and 3. For other geometric configurations see ref. 2, 3, 5 and 7. The first wall radius will be 3 m and the fusion power will be 4200 MW appropriate to a 2 GWe plant, a reasonable size plant for 30 years from now—the assumed time for introduction of large numbers of plants. The neutron wall load is 30 MW/m^2 on the liquid. The lifetime of the structures behind this liquid is the life of the plant. The transit time for the liquid is estimated at 0.3 s. There are only three candidate liquids that might meet all the criteria, especially being able to breed enough tritium, Li, Flibe and $Li_{17}Pb_{83}$. There are two typical formulation of Flibe: Li_2BeF_4 and $LiBeF_3$. The first has a ten times lower viscosity but a melting point of 460 °C and the second has a melting point of 360 °C. For now we take the first formulation for our examples, however, the second needs to be reevaluated from time to time. The density of the vapor over the liquid at equilibrium is given in Fig. 4 for the three liquids. All three appear to be possible

candidates, each with its advantages and disadvantages. The extra high Z of Pb in $Li_{17}Pb_{83}$ is especially worrisome in that very little impurity is allowed.

In the examples, we consider steady state cases but we need to remember the bias towards steady state is built up on intuition based in large part on experience with the Tokamak. The use of liquids with its large heat storing capacity reduces the need for steady state and in a pulsed design the evaporated material takes considerable time to penetrate the burning plasma (~1 sec for usual MFE like conditions). If the burn is over in much under a second the contamination takes on a different characteristic, i.e., can the evaporated material be removed before the next pulse? In an IFE plant, the power is pulsed several times a second. The cyclic fatigue and clearing the chamber for the next shot appear manageable.

The evaporation rate is given in Fig. 5. The assumption is the evaporation is an equilibrium process. Corrections would be needed when the rate is such that the surface gets depleted in the more volatile species, BeF_2 or Pb in the case of Flibe or $Li_{17}Pb_{83}$. Also the primary evaporating species in $Li_{17}Pb_{83}$ is Pb because the lithium is chemically active and is tightly bound. This correction should not be important for temperatures below 640 and 700 °C for Li_2BeF_4 and $Li_{17}Pb_{83}$. When there are sufficient collisions of the evaporated material so that the local pressure is enhanced, the evaporation rate would be reduced somewhat; this occurs at approximately 720, 860 and 980 °C for Li, Li_2BeF_4 and $Li_{17}Pb_{83}$. When the evaporative cooling becomes important the rate again would be diminished; this occurs at approximately 750, 910 and 990 °C for Li, Li_2BeF_4 and $Li_{17}Pb_{83}$.

The evaporation is a local effect depending on the surface temperature. Therefore, it is important to be able to predict the surface temperature on a fluid element facing the plasma as it moves from the inlet to the outlet. The outlet temperature should be kept below any materials limits and the inlet must be amply above the melting point to avoid freeze up in the heat exchangers. The energy striking the liquid surface will heat it. This energy comes in the form of radiation (bremsstrahlung, cyclotron, optical excitation and recombination) and neutral particles. The charged particle power carried out of the plasma is assumed to efficiently flow out along the open field lines and not strike the liquid surface. There is some charge exchange produced neutrals that will strike the liquid wall causing sputtering and more heating of the surface, however, these effects have been assumed negligible. The bremsstrahlung radiation penetrates deeply into the liquid and only part of this radiation raises the temperature of the surface. The cyclotron radiation is ignored because with conducting liquids, most of it is reflected and little is absorbed and in the case of Flibe most of it penetrates deeply and doesn't contribute much to heating the surface.

The temperature of the liquid surface is given below:

$$T_{outlet} = T_{inlet} + \Delta T \quad (1)$$

$$\Delta T = 2qf\sqrt{\frac{\tau}{\pi k \rho C_p}} \quad (2)$$

$$f = 1 - e^{-x/\lambda} \quad (3)$$

The power per unit area on the surfaces is q. The thermal diffusion distance is x, the distance heat can diffuse in a time, τ, the time the liquid is being heated, i.e., its transit time ~0.3 s. For 0.3 s the thermal diffusion distance, x, is 2.6 mm, 0.22 mm and 2.5 mm for Li, Flibe and $Li_{17}Pb_{83}$. The mean free paths of photons, λ, for the three liquids is given[8] in Fig. 6. The deep penetration factor, f, is calculated by Eq. 3 and plotted in Fig. 7 and 8 and is simply the fraction of energy deposited within a thermal diffusion distance of the surface. We can see that for Li most of the radiation is deep penetrating for Te greater than 7 keV and for a typical temperature of 13 keV, f is 0.03. For Flibe at 13 keV, f is 0.13. $Li_{17}Pb_{83}$ gets no advantage of deep penetration as can be seen in Fig. 8. The assumption is there is no convection of the liquid as it moves through the chamber. Convection (turbulence) would lower the temperature rise and surely must occur some which would lower the evaporation rates estimated below.

Typical parameters are taken from ITER examples[9, 10]. $T_{e,ave.} = 12.8$ keV, $P_{Brem} = 0.03 \times P_{fus}$; $P_{optical} = 0.01 \times P_{fus}$; $P_{cyclotron} = 0.004 \times P_{fus}$. For a sphere of 3 m radius and 4200 MW_{fus} and an area of 113 m^2, the bremsstrahlung power is 1.1 MW/m^2, is 0.37 MW/m^2 and cyclotron which is ignored for the reasons stated earlier is 0.15 MW/m^2. Plugging these numbers in the equations above we get the results shown in Table 1.

Table 1
Temperature rise of liquid as it passes through the chamber

	$\Delta T_{with\ deep\ penetration}$	$\Delta T_{without\ deep\ penetration}$
Li	26 °C	91
Flibe	164	463
$Li_{17}Pb_{83}$	140	140

Christofolos[1] ignored the surface temperature rise but as we can see from Table 1 his assumption for lithium was reasonable but the correction for Flibe and $Li_{17}Pb_{83}$ is large.

For the purpose of calculating the amount of evaporation, the fluid surface is divided into five equal zones. The temperature rise for each is calculated and the

evaporation for each is calculated and then added up. This is done to account for the strongly rising evaporation rate with temperature. The assumed inlet temperature was 380 °C, 500 °C, and 400 °C for Li, Flibe and $Li_{17}Pb_{83}$. It would be possible to introduce an extra cool layer of liquid on the surface and have the bulk liquid at a higher temperature, but this was not done. The penetration assumes all radiation comes at Te and all perpendicular to the liquid surface. A more accurate treatment would integrate over the bremsstrahlung energy spectra and over angles of photons striking the liquid surface. The results are 0.96×10^{23}/s of Li for Li, 0.037×10^{23}/s of BeF_2 for Flibe, and 0.13×10^{23}/ of Pb for $Li_{17}Pb_{83}$. The power needed to ionize this vapor at a nominal 50 eV per ion pair is 0.78, 0.03 and 0.1 MW for Li, Flibe and $Li_{17}Pb_{83}$. This is very manageable and in fact is a small fraction of the alpha particle power which will largely be in the form of a flowing edge plasma outside of the separatrix and available to do this ionizing. However, we want to very efficiently ionize evaporated material so as to prevent contamination as will be discussed below.

We will now estimate the allowed evaporation rate. In the ITER computer run[9] the ratio n_α/n_e=0.1. I am going to make an assumption that in the burning plasma the allowed impurity levels are:

$n_{Li}/n_e =$ 0.05 $Z_{ave.} = 3$
$n_{Flibe}/n_e =$ 0.005 $Z_{ave.} = 7.3$ for BeF_2
$n_{Li_{17}Pb_{83}}/n_e = 0.0001$ $Z_{ave.} = 82$ for Pb

Assume the impurity lifetime (being edge fed) is 1 s and the alpha lifetime is 13 s. The fraction of evaporated particles that is allowed to enter the hot plasma is defined as $F_{allowed}$. $F_{allowed}$ is the allowed rate of vapor impinging on the separatrix divided by the evaporation rate. The allowed impurity impingement rate to the edge of the burning plasma at the separatrix and the $F_{allowed}$ factors are given below.

$$\dot{N}_{Li} = (n_{Li}/n_e)\,(n_e/n_\alpha)\dot{N}_\alpha$$
$$= 0.05 \times (1/0.1) \times 1.4\times10^{21}/s$$
$$= 0.7\times10^{21}/s \quad \text{allowed}$$

$$\dot{N}_{Li} = 0.96\times10^{23}/s \quad \text{evaporation}$$

$$F_{allowed} = (0.7\times10^{21}/s)/(0.96\times10^{23}/s)$$
$$= 7.3\times10^{-3}$$

$$\dot{N}_{Flibe} = (n_{Flibe}/n_e)\,(n_e/n_\alpha)\dot{N}_\alpha$$

$= 0.005 \times (1/0.1) \times 1.4\times10^{21}/s$

$= 0.07\times10^{21}/s$ allowed

$\dot{N}_{Flibe} = 0.92 \times10^{23}/s$ evaporation

$F_{allowed} = (0.07\times10^{21}/s)/(0.037 \times10^{23}/s)$

$= 1.9\times10^{-2}$

$\dot{N}_{\alpha} = 1.4\times10^{21}/s$, which corresponds to the helium production rate for 2 GWe

$\dot{N}_{Li17Pb83} = n_{Li17Pb83}/n_e\,(n_e/n_{\alpha})\dot{N}_{\alpha}$

$= 0.0001 \times (1/0.1) \times 1.4\times10^{21}/s$

$= 1.4\times10^{18}/s$ allowed

$\dot{N}_{Li17Pb83} = 1.33 \times10^{22}/s$ evaporation

$F_{allowed} = (1.4\times10^{18}/s)/(1.33\times10^{22}/s)$

$= 1.05\times10^{-4}$

Ability of the edge plasma to ionize evaporating atoms or molecule

The evaporating atoms or molecules will have to avoid ionization in the edge plasma in order to penetrate into the hot confined plasma and contribute to impurity buildup. Once ionization occurs in the edge plasma the opportunity exists for the species to be swept out along the open field lines into a dump region where they can strike a surface and be pumped. There is a complex set of phenomena taking place in the edge plasma for which further analysis using modern computer codes such as UEDGE would be useful. Here we present an estimate of the problem by assuming the evaporating species comes off perpendicular to the surface at the thermal speed, v_o, and has a probability of attenuation, $F_{attenuation}$ given below.

$T_{edge} = 0.4$ keV

$n_e = 4\times10^{13}$ cm^{-3} at separatrix

$\sigma v_e \sim 3\times10^{-8}$ cm^3/s

L = 1 cm = average thickness of edge plasma

$F_{attenuation} = \exp-(Ln_e\sigma v_e/v_o)$

Table 2
Predicted ionizing ability of the edge plasma

	Li	Flibe	$Li_{17}Pb_{83}$
$F_{attenuation}$	2.1×10^{-4}	3.7×10^{-9}	9.5×10^{-20}
v_o; m/s	1420	618	274
Temperature, K	666	855	743
$F_{allowed}$	7.3×10^{-3}	1.9×10^{-2}	1.1×10^{-4}

The temperature of the liquid surface half way through the chamber is given in Table 2. The efficiency of ionizing this evaporating material that is needed to achieve the above allowed impurity influxes and therefore the steady state allowed impurity levels is 0.9927, 0.98, and 0.9999 (inefficiency or penetration factors are 7.3×10^{-3}, 1.9×10^{-2}, and 1.1×10^{-4} and is equal to 1 - $F_{allowed}$) for Li, Flibe and $Li_{17}Pb_{83}$. From Table 2 we see the ionizing ability of the edge plasma is sufficient to adequately prevent penetration of the atoms or molecules across the separatrix. The question of charged particle diffusion across the edge plasma before the impurity is exhausted along the field lines, needs to be examined. Stated another way, in the time this particle gets swept out to the pumping (condensing) region, how many first diffuse across the separatrix? Edge particle transport calculations are needed.

Discussion

Much work needs to be done to have a self-consistent feasible design for a liquid protected wall chamber for magnetic fusion. The configuration of liquid for a Tokamak or toroidal pinch shown in Fig. 1 does not look hopeful because the lack of a good place for the edge plasma to be exhausted and the need for penetrations through the liquid. The field reversed configuration looks quite hopeful as shown in Fig. 2. Conducting liquid metal can be flown along field lines for the most part and help in stabilizing the tilt instability. Short-fat versions as shown or long-slender versions not shown are possible. More work should be done on these configurations including self-consistent magnetic fields and MHD effects on the liquid flow. Spheromak and short-fat FRC configurations can use the flow pattern shown in Fig. 3. Spinning chamber would walls help guide the liquid and centrifugal forces will help keep the liquid out of the edge plasma region. Configurations that use moving metal parts in a magnetic field will require extra design to avoid problems with induced currents. Mechanisms with seals and bearings have been worked as shown in Fig. 9 and are applicable to that of Fig. 3. The liquid can be non-conducting as in the case of Flibe or with much MHD complication a conducting liquid metal can be used. Clearly more work is needed. The role of conducting walls behind the Flibe or conducting liquid metal in the two classes of liquid needs much study relative to stability of

the plasma. This paper is intended to introduce the ideas and motivation further work. Clearly much further work is needed before a feasible design emerges.

Conclusions

When proper accounting of the deep penetration of bremsstrahlung radiation is taken into account the evaporation while large can be sufficiently screened from penetrating into the burning plasma by ionization in the edge plasma. The impurity concentration has been estimated to reach a steady state value that is adequately low. The power to ionize the evaporated liquid is low and the ability of the edge plasma to ionize enough of the evaporated material is adequate. More work is needed to refine and check the calculations given in this paper. The use of flowing liquid walls for magnetic fusion systems appears feasible. There are a number of profound advantages with the use of liquid walls: lower the cost of electricity by >35%; remove the need to develop first wall materials saving >4B$ in development; reduce the amount and kind of wastes generated in the plant; permit a wider choice of materials. The advantages are so profound that more work should be carried out on liquid walls for magnetic fusion system. The nature of this work is to adapt the geometric and topological constraints of flowing liquids to the plasma containment requirements, magnet locations, heating systems and so forth.

Acknowledgments

Useful discussion are appreciated with Ken Fowler, Scott Haney, Charles Hartman, Bick Hooper, Tom Rognlien, and L. M. Sevigny.

References

1. N. C. Christofilos, "Design for a High Power-Density Astron Reactor," J. Fusion Energy 8 (1989) 97-105.

2. R. W. Moir, "Rotating Liquid Blanket for a Toroidal Fusion Reactor", *Fusion Engineering and Design* 5 269 (1987).

3. R. W. Moir, "The Logic Behind Thick, Liquid-Walled, Fusion Concepts," Nuclear Engineering and Design 29 (1995) 34-42.

4. W. M. Wells, "A system for handling diverter ion and energy flux based on a lithium droplet cloud," Nuclear Technology/Fusion 1 (1981) 120-127.

5. Ralph W. Moir, "The High-Yield Lithium-Injection Fusion-Energy (HYLIFE)-II inertial fusion energy (IFE) power plant concept and implications for IFE," Physics of Plasmas 2 (6) (1995).

6. R. W. Moir, "Rotating Liquid Blanket with No First Wall for Fusion Reactor", *Fusion Technology* 15 674 (1989).

7. R. Burke, "Argonne National Lab Design Activities", p. 5-16, ANL-79-41, Proc. of Heavy Ion Fusion Workshop, Argonne National Laboratory, Sept. 19-26, 1978, Argonne, Ill.

8. D. E. Cullen et al, "Tables and Graphs of Photon-interaction cross sections from 10 eV to 100 GeV derived from the LLNL Evaluated photon data library (EPDL) Part A: Z=1 to 50," UCRL-5000400, Vol. 6 Part A. Rev. 4 (1989).

9. Scott Haney, Private communications and his ITER printout of 4/18/95.

10. J. D. Galambos, L. J. Perkins, S. W. Haney, and J. Mandrekas, "Commercial Tokamak reactor potential with advanced Tokamak operation," Nuclear Fusion 35 (1995) 551-573..

Figure Captions

Fig. 1. Schematic of rotating liquid blanket for the Tokamak. The liquid considered was $LiBeF_3$.

Fig. 2. Field reversed configuration (from ref. 1) allows conducting liquid to flow vertically downward along field lines.

Fig. 3. A nonconducting liquid can be made to almost completely surround a region by creating artificial gravity by spinning the liquid as shown in the above schematic drawing. Magnet coils are not shown. The moving parts and seals needed here are shown in detail in Fig. 9.

Fig. 4. The density of the vapor over the three candidate liquids at equilibrium versus temperature is given.

Fig. 5. The rate of evaporation is given. For Flibe the evaporating species is over 90% BeF_2 and less than 10% LiF. For $Li_{17}Pb_{83}$ the volatile evaporating species is over 95% Pb and less than 5 % Li .

Fig. 6. The photon mean free path versus energy is plotted from Ref. 8.

Fig. 7. The deep penetration factor, fraction of energy deposited within one thermal diffusion distance, is plotted versus electron temperature. The oversimplified assumption is the radiation strikes normal to the surface and the photons are given off at their average energy, Te, rather than with a distribution ($e^{-E/Te}$).

Fig. 8. The deep penetration factor is not interesting for $Li_{17}Pb_{83}$ for Te less than 500 keV.

Fig. 9. An example of a spinning liquid apparatus for flowing liquids shows motors, seals and so forth. This configuration might be usefully adapted to several magnetic confinement configurations such as the Z-Pinch and the long-slender field reversed configuration. The figure is from Ref. 7, "The Argonne Heavy-Ion-Beam Reactor using a centrifugal blanket."

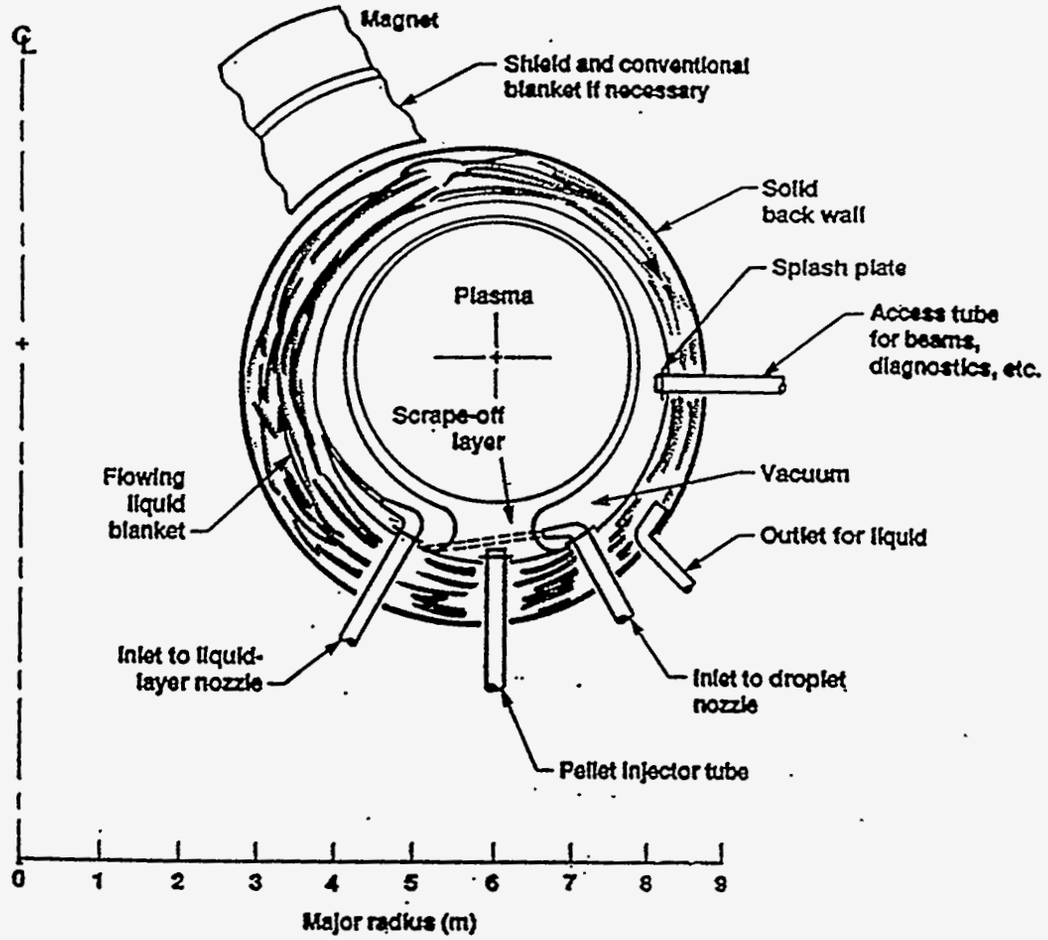

Fig. 1. Schematic of rotating liquid blanket for the Tokamak. The liquid considered was $LiBeF_3$.

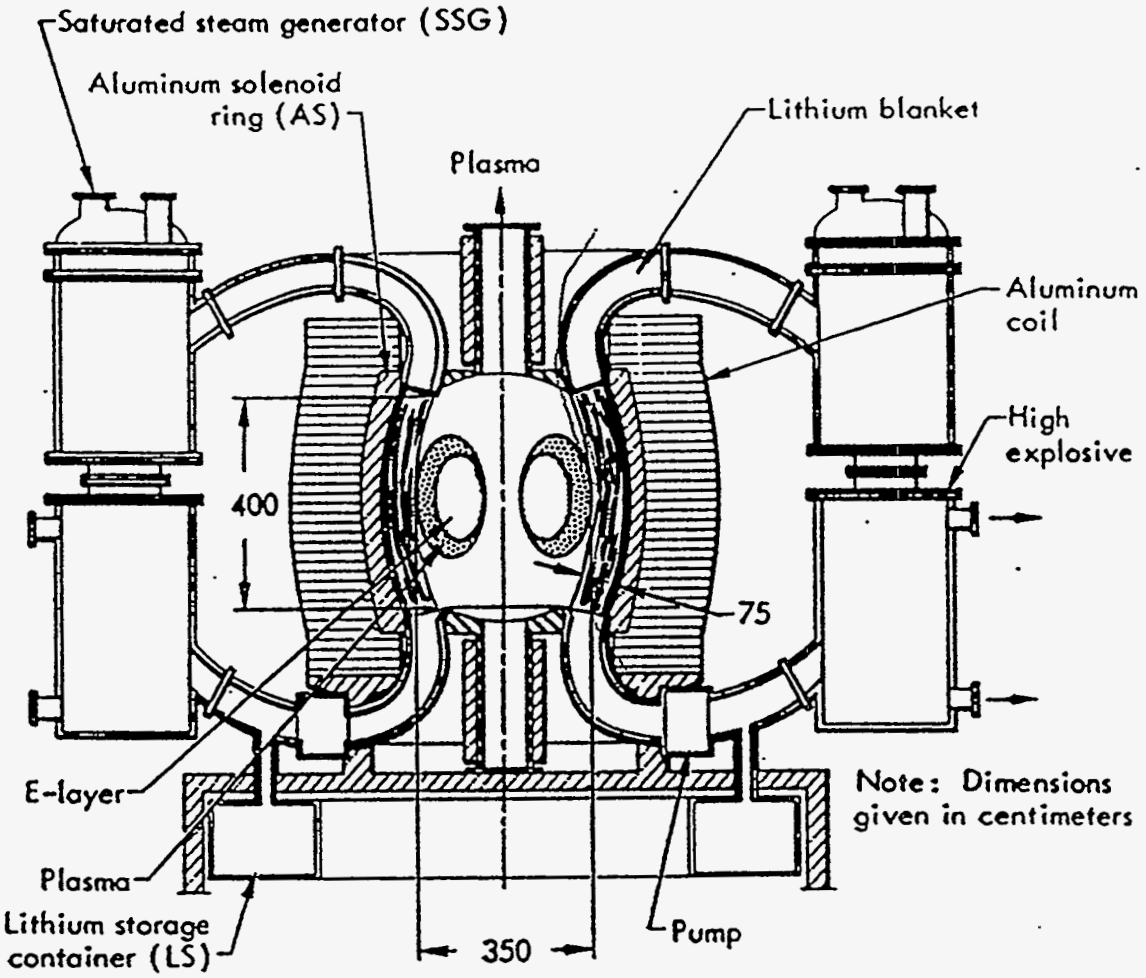

Fig. 2. Field reversed configuration (from ref. 1) allows conducting liquid to flow vertically downward along field lines.

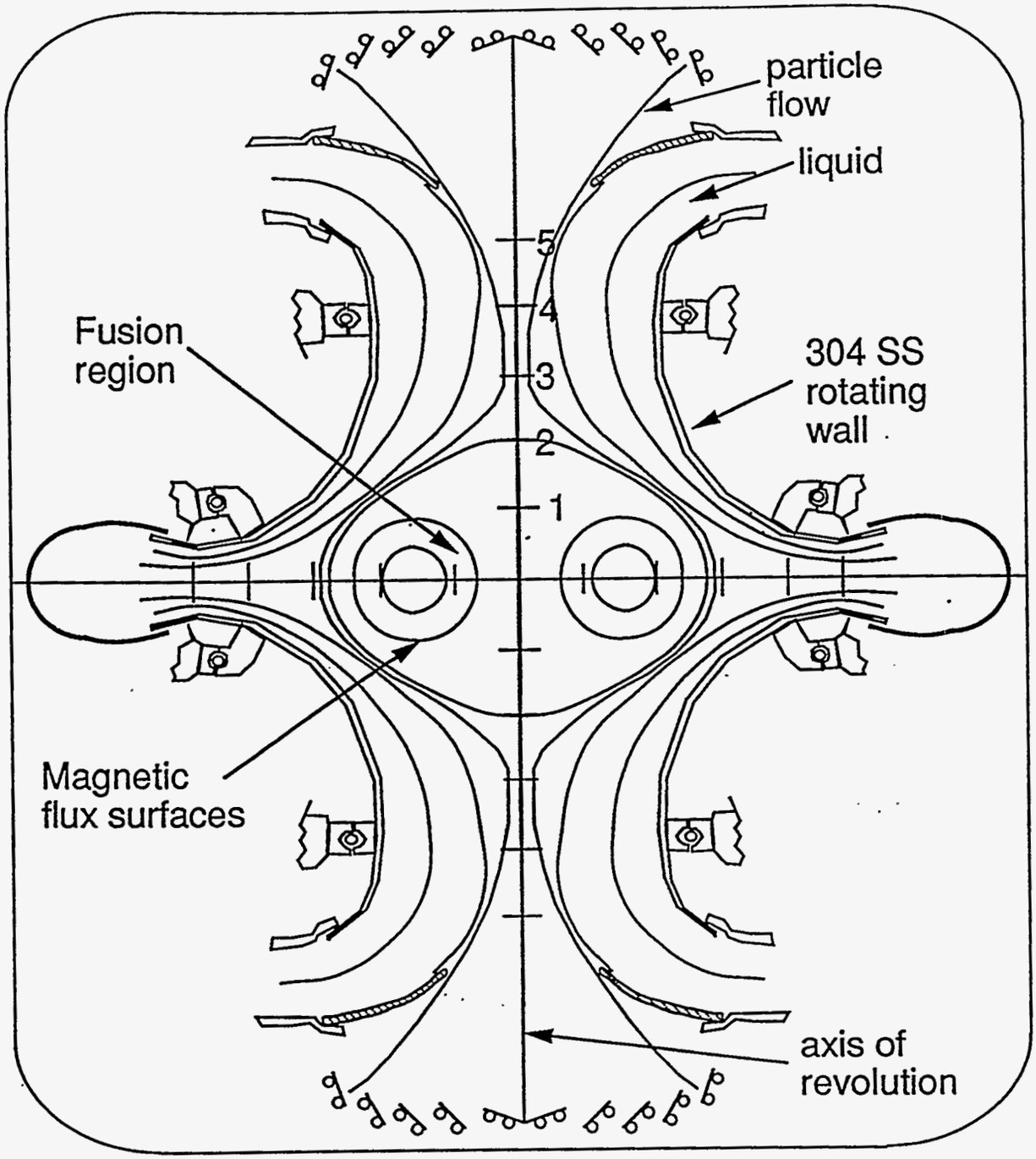

Fig. 3. A nonconducting liquid can be made to almost completely surround a region by creating artificial gravity by spinning the liquid as shown in the above schematic drawing. Magnet coils are not shown. The moving parts and seals needed here are shown in detail in Fig. 9.

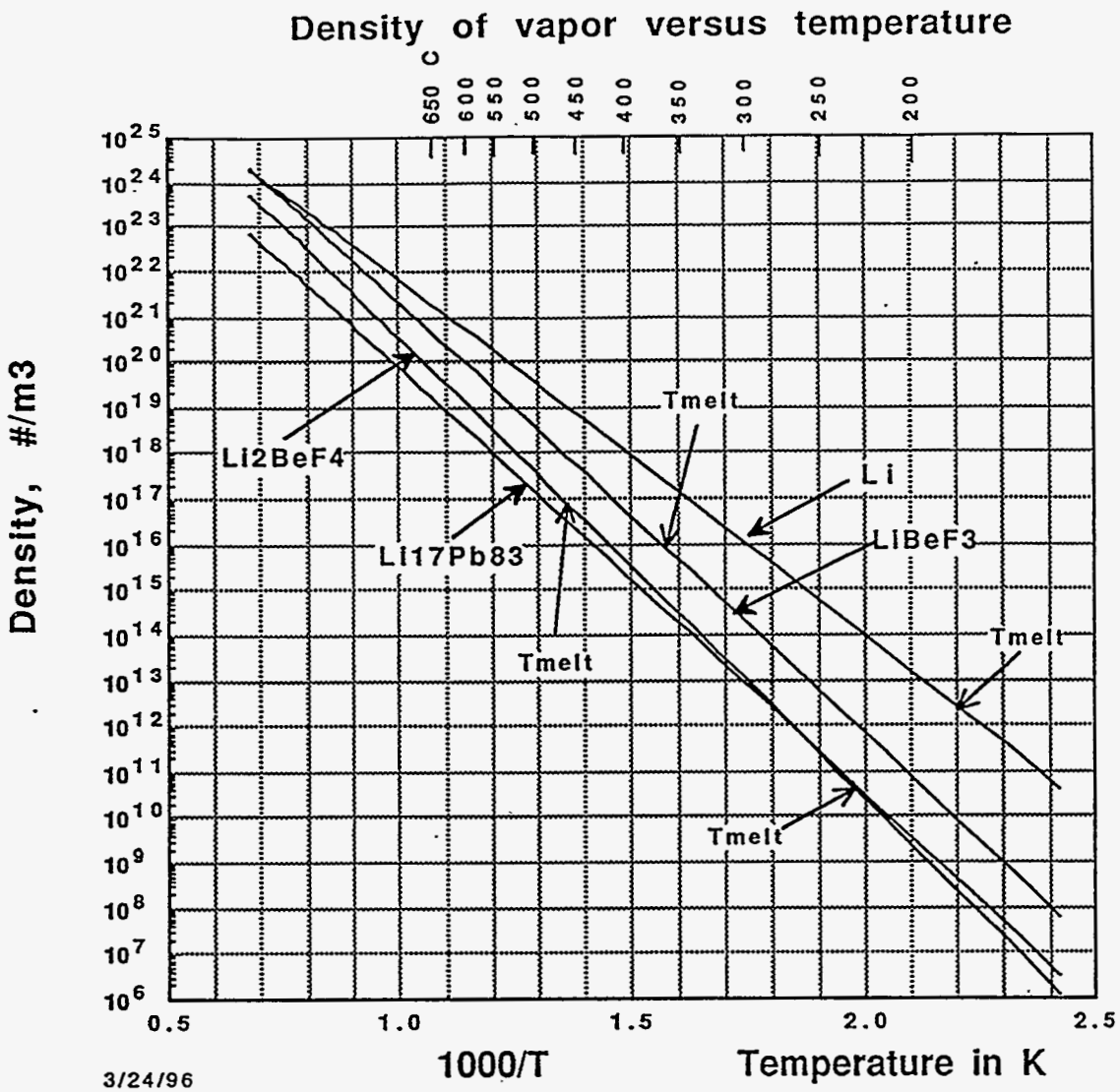

Fig. 4. The density of the vapor over the three candidate liquids at equilibrium versus temperature is given.

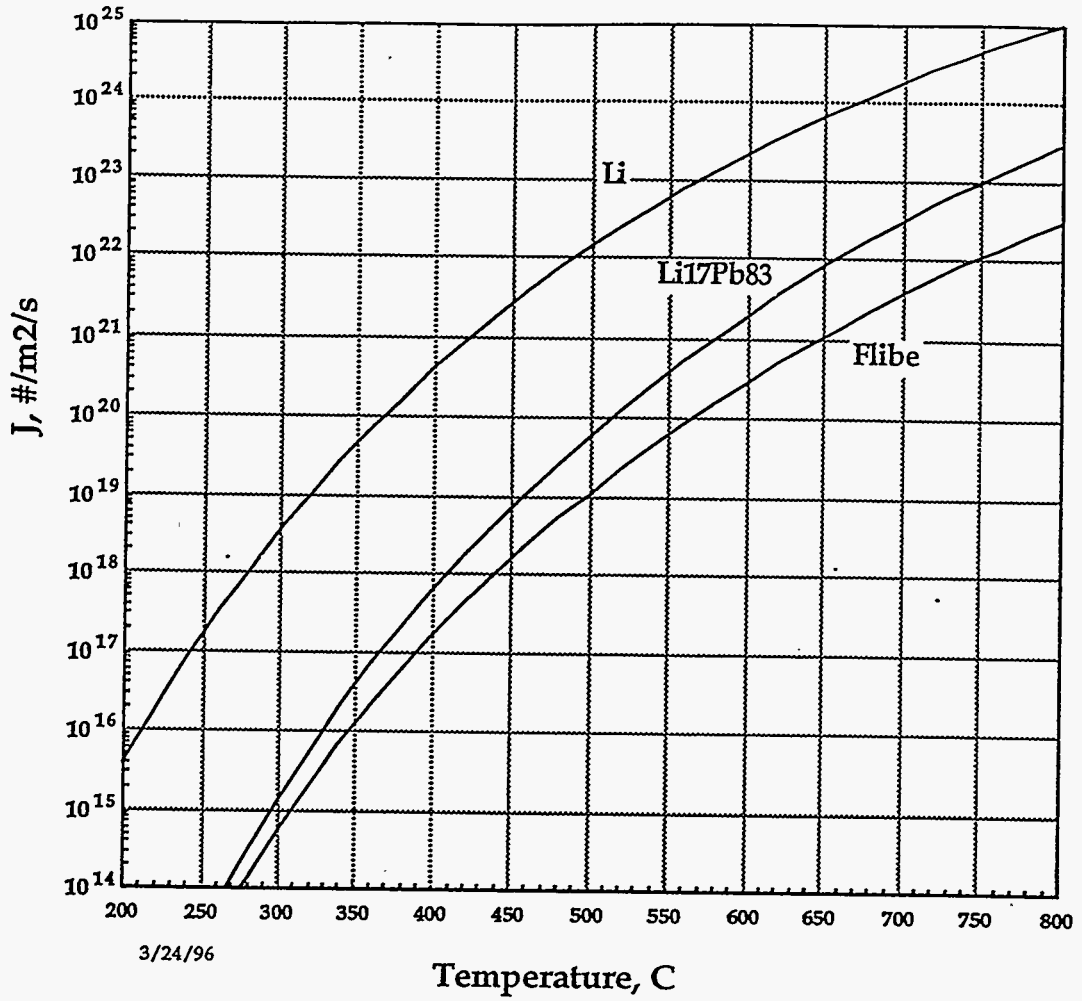

Fig. 5. The rate of evaporation is given. For Flibe the evaporating species is over 90% BeF_2 and less than 10% LiF. For $Li_{17}Pb_{83}$ the volatile evaporating species is over 95% Pb and less than 5 % Li .

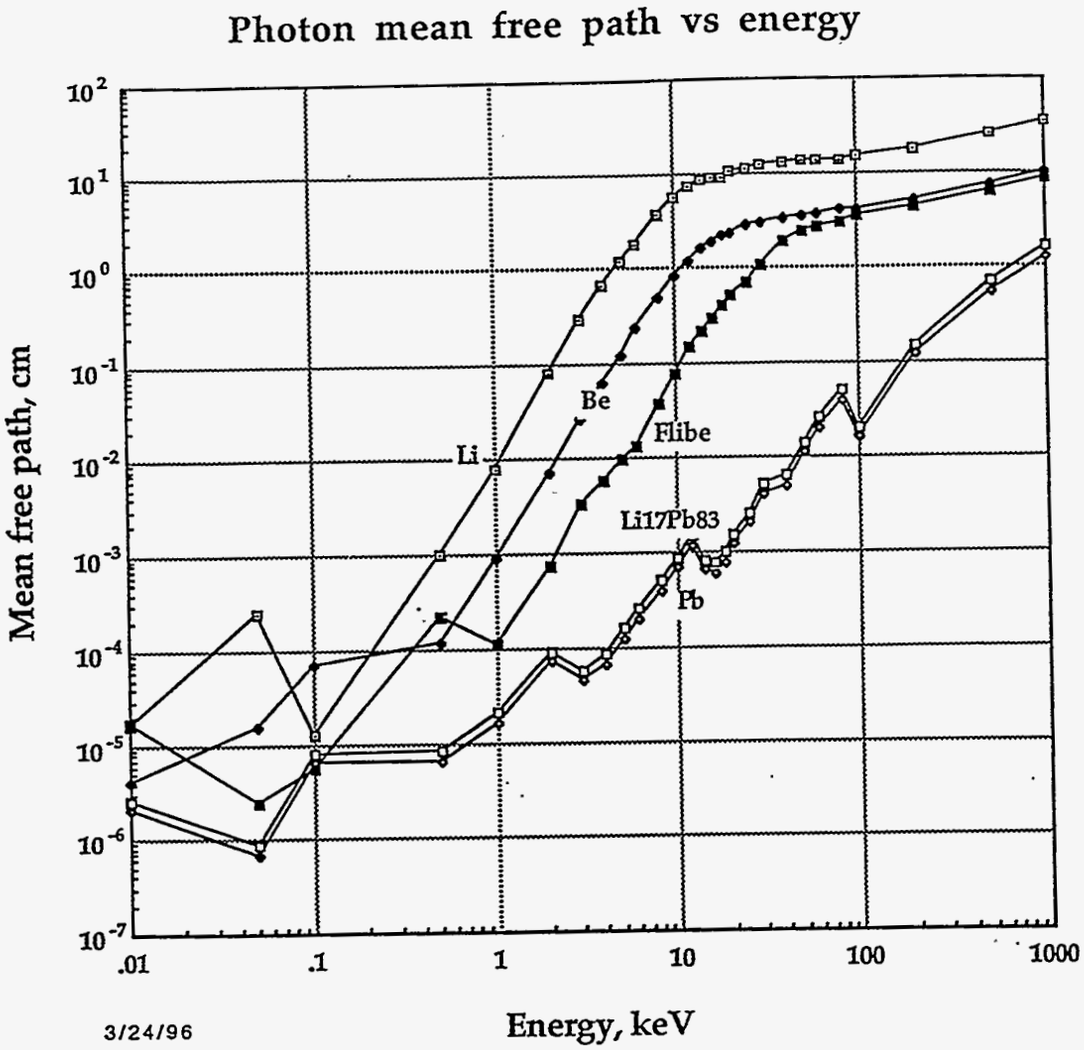

Fig. 6. The photon mean free path versus energy is plotted from Ref. 8.

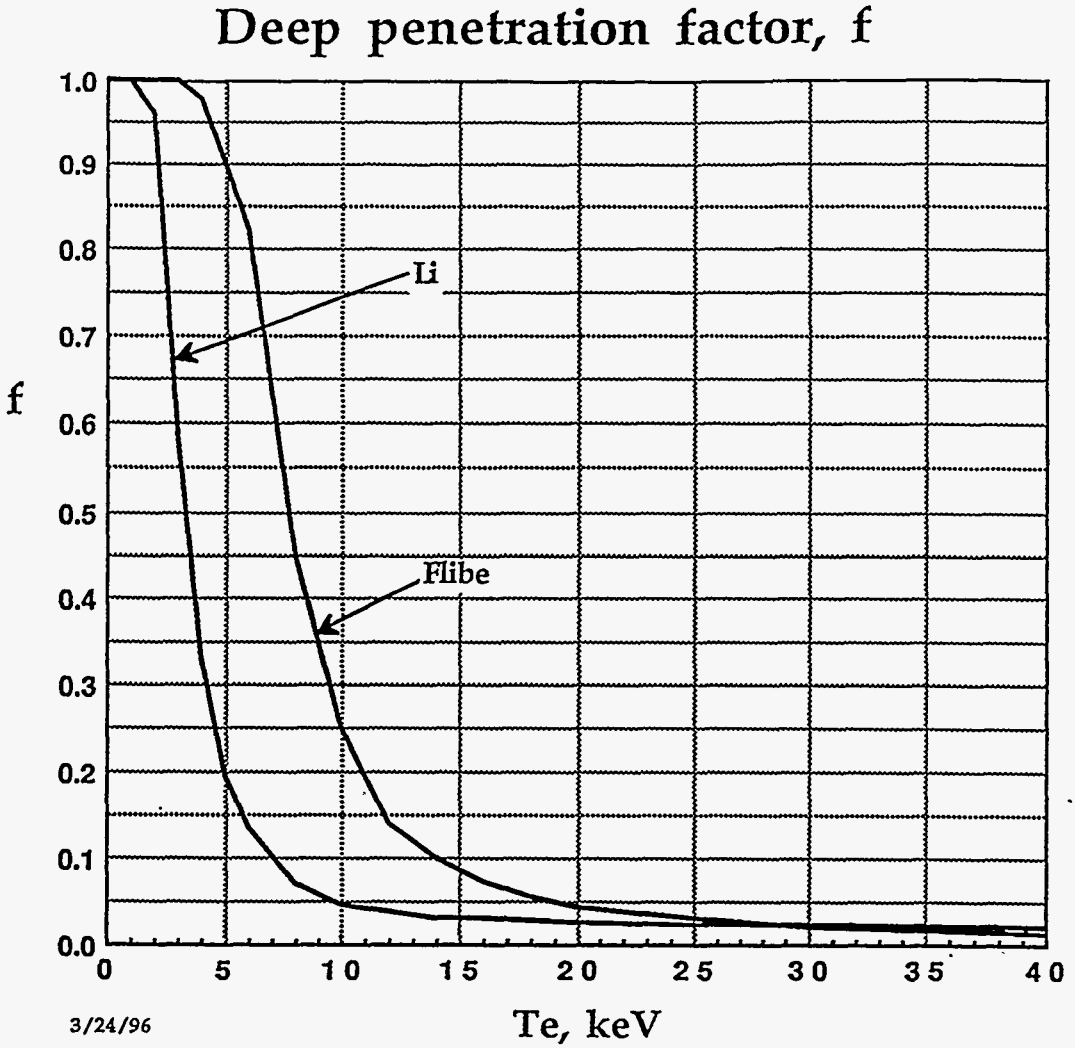

Fig. 7. The deep penetration factor, fraction of energy deposited within one thermal diffusion distance, is plotted versus electron temperature. The oversimplified assumption is the radiation strikes normal to the surface and the photons are given off at their average energy, Te, rather than with a distribution ($e^{-E/Te}$).

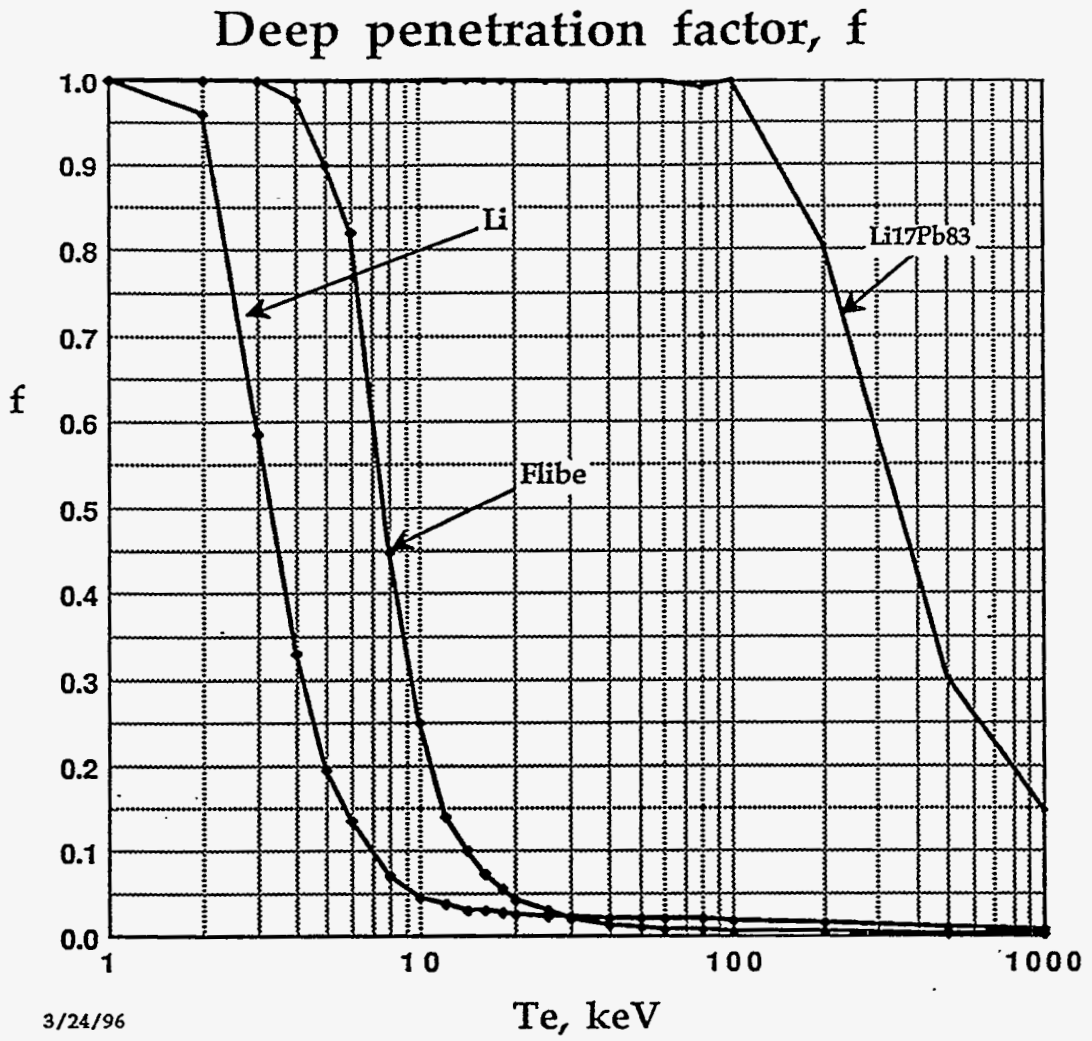

Fig. 8. The deep penetration factor is not interesting for $Li_{17}Pb_{83}$ for Te less than 500 keV.

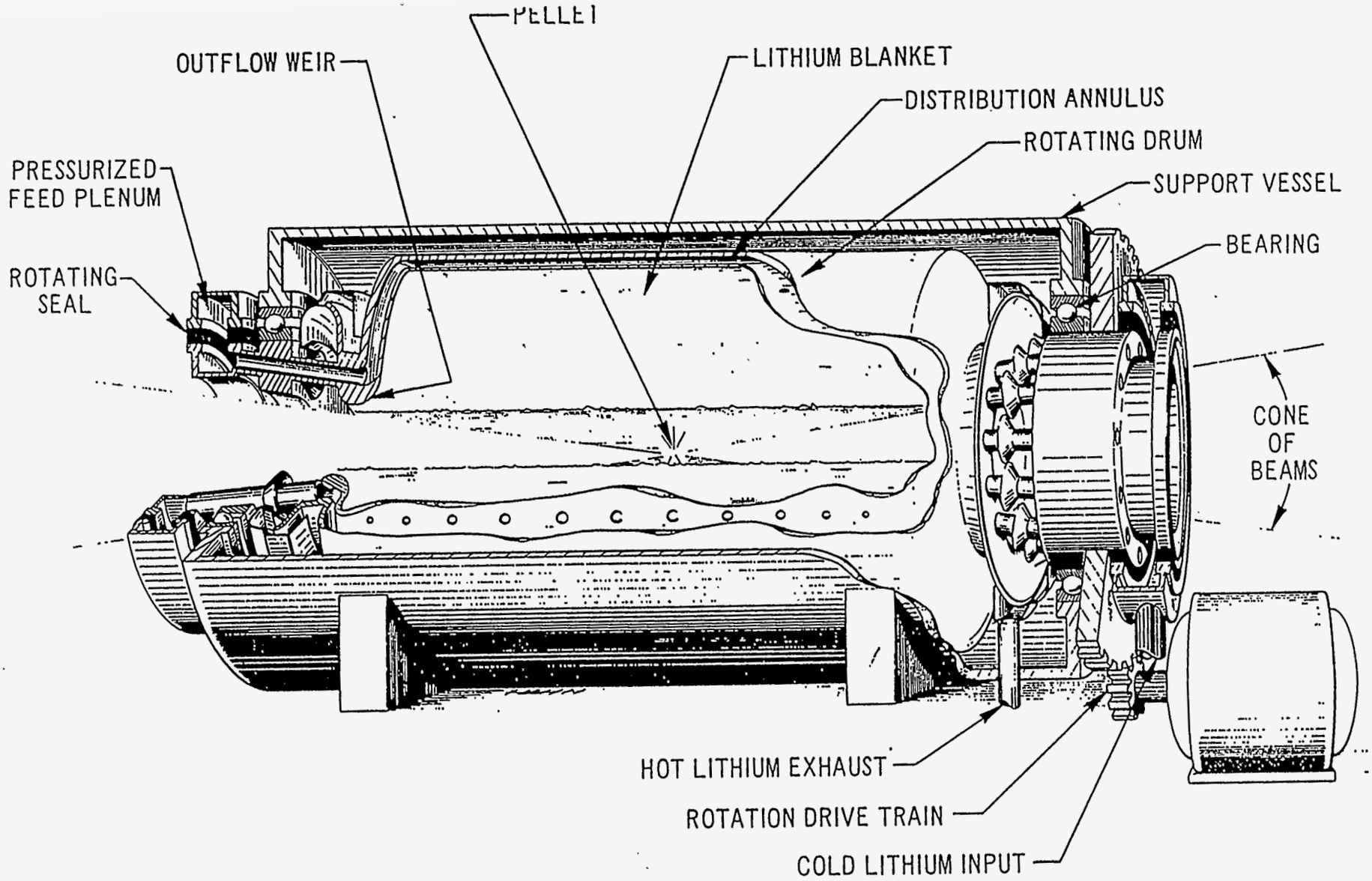

Fig. 9. An example of a spinning liquid apparatus for flowing liquids shows motors, seals and so forth. This configuration might be usefully adapted to several magnetic confinement configurations such as the Z-Pinch and the long-slender field reversed configuration. The figure is from Ref. 7, "The Argonne Heavy-Ion-Beam Reactor using a centrifugal blanket."